# Neutron Radii of Calcium Isotopes from Pion Total Cross Section Measurements*

M. J. Jakobson, G. R. Burleson, J. R. Calarco, M. D. Cooper, D. C. Hagerman, I. Halpern, R. H. Jeppeson, K. F. Johnson, L. D. Knutson, R. E. Marrs, H. O. Meyer, and R. P. Redwine

*University of Montana, Missoula, Montana 59801, and California Institute of Technology, Pasadena, California 91109, and Los Alamos Scientific Laboratory, Los Alamos, New Mexico 87545, and New Mexico State University, Las Cruces, New Mexico 88003, and Stanford University, Palo Alto, California 94305, and University of Basel, Basel, Switzerland, and University of Washington, Seattle, Washington 98195, and University of Wisconsin, Madison, Wisconsin 53706*

(Received 7 April 1977)

Measurements of the total cross section differences $\sigma_T(^{48}\mathrm{Ca}) - \sigma_T(^{40}\mathrm{Ca})$ and $\sigma_T(^{44}\mathrm{Ca}) - \sigma_T(^{40}\mathrm{Ca})$ are reported for positive and negative pions. Optical-model calculations are used to extract values of the rms neutron radius difference for each isotope pair. For $^{48}\mathrm{Ca}$-$^{40}\mathrm{Ca}$ the deduced radius difference agrees with the results of recent $\alpha$-particle and proton scattering experiments but is smaller than values predicted from Hartree-Fock calculations.

Measurements of the proton and neutron density in nuclei provide a means for testing nuclear many-body theories such as Hartree-Fock. These calculations are now quite sophisticated, and should be especially reliable for closed-shell nuclei such as $^{40}\mathrm{Ca}$ and $^{48}\mathrm{Ca}$. In this Letter we describe a method for obtaining information about neutron density distributions from measurements of pion total cross sections at energies near the (3, 3) $\pi$-nucleon resonance. In this energy region the $\pi$-nucleus interaction has two important features. First, the pions are strongly absorbed. As a result one can obtain an adequate description of the interaction from relatively simple models. Second, negative (positive) pions couple more strongly to neutrons (protons). This enhances the sensitivity of the $\pi^-$ cross section to the neutron radius.

We report here total cross section results for positive and negative pions on $^{40}\mathrm{Ca}$, $^{44}\mathrm{Ca}$, and $^{48}\mathrm{Ca}$ for energies ranging from 90 to 240 MeV. In order to reduce systematic errors, we consider only the cross section differences between pairs of isotopes. By comparing the measurements with the results of optical-model calculations we extract values of $\Delta R_n$, the rms neutron radius difference, and $\Delta R_p$, the rms proton radius difference, for each isotope pair. The extracted $\Delta R_p$ values provide a consistency check on the method, since these quantities are well known. As further evidence that our analysis is reasonable, we demonstrate that calculated total cross section differences are insensitive to many details in the calculation. We conclude by comparing our values of $\Delta R_n$ with the results obtained in other experiments and with Hartree-Fock calculations.

The measurements were carried out at the low-energy pion channel[1] at Clinton P. Anderson Meson Physics Facility (LAMPF) using a beam-attenuation technique.[2] A complete description of the experiment will be given in a subsequent paper. Incident pions were individually detected and counted by plastic scintillators upstream of the target assembly while protons, muons, and electrons were rejected with a differential Cherenkov counter.[3] The resulting beam contained about $10^3$ tagged pions/sec (time averaged) confined to a beam spot 2.7 cm in diameter. The spatial distribution of the beam was monitored with multiwire proportional chambers. The relatively high intensity and small spot size made it possible to use rare isotopes such as $^{48}\mathrm{Ca}$ as targets. The targets were approximately 1.5 g/cm$^2$ thick and were fabricated to be nearly identical. To insure that the measurements for the three isotopes were obtained under similar experimental conditions, the targets were cycled every 2 min. Downstream from the target, pions were detected with a stack of ten concentric disk-shaped plastic scintillators centered on the beam axis. With each counter one measures the cross section for all processes for which no charged particles hit the scintillator. In order to subtract the cross section which arises from Coulomb scattering we write the elastic scattering amplitude as $f = f_c + f_n$, where $f_c$ is the scattering amplitude for point charges. The total cross section is then defined as

$$\sigma_T = \sigma_R + \int_{4\pi} |f_n|^2 d\Omega, \tag{1}$$

where $\sigma_R$ is the reaction cross section. Experi-

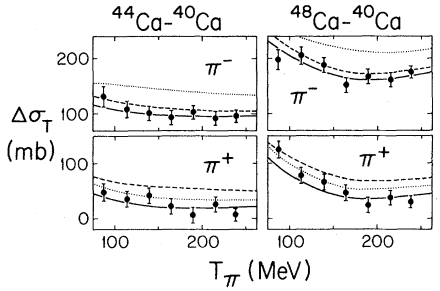


FIG. 1. Total cross section differences for $\pi^+$ and $\pi^-$ on Ca isotopes. The solid curves are fits obtained by adjusting $\Delta R_n$ and $\Delta R_p$. The dotted (dashed) curves show the effect of increasing $\Delta R_n$ ($\Delta R_p$) by 0.1 fm.

mentally, $\sigma_T$ is obtained by subtracting the Coulomb and Coulomb-nuclear interference contributions[4] from the measured cross sections and then extrapolating to zero solid angle.

The measured total cross section differences and their statistical errors are shown in Fig. 1. The curves in Fig. 1 were calculated using the Kisslinger optical model.[5,6] This model is based on the impulse approximation in which the optical potential depends linearly on the nucleon density and is directly proportional to the strength of the $\pi$-nucleon transition amplitude.[7] Woods-Saxon shapes were assumed for the neutron and proton densities. The solid curves were obtained by treating $\Delta R_n$ and $\Delta R_p$ as free parameters which were adjusted to fit the $\pi^-$ and $\pi^+$ data points above 125 MeV. The results[8] are given in Table I.

Before discussing the significance of these results we consider the systematic errors involved in extracting $\Delta R_n$ and $\Delta R_p$. The sensitivity of $\Delta\sigma_T$ to changes in $\Delta R_n$ and $\Delta R_p$ is illustrated in Fig. 1. The dashed curves show the effect of increasing $\Delta R_p$ by 0.1 fm over the best-fit value. Similarly a comparison of the dotted curves with the solid curves shows the effect of a 0.1-fm increase in $\Delta R_n$. Typically, a 0.01-fm change in $\Delta R_n$ corresponds to a 4.5 mb (1.5 mb) change in $\Delta\sigma_T$ for $\pi^-$ ($\pi^+$). A 0.01-fm change in $\Delta R_p$ corresponds to a 1-mb (3 mb) change in $\Delta\sigma_T$ for $\pi^-(\pi^+)$.

In our analysis we use the optical model to extract values of $\Delta R$, and thus it is important to show that the model accurately predicts the cross section *differences*. We achieve this end by demonstrating that a wide variety of models predict values of $\Delta\sigma_T$ which are nearly identical. Calculations of $\Delta\sigma_T$ for $\pi^-$ on $^{48}$Ca and $^{40}$Ca obtained with four different models are shown in Fig. 2(a). The dot-dashed curve corresponds to a Glauber

TABLE I. Experimental values of $\Delta R_p$ and $\Delta R_n$.

| Particle | Ref. | $^{44}$Ca-$^{40}$Ca | $^{48}$Ca-$^{40}$Ca |
|---|---|---|---|
| | | $\Delta R_p$ (fm) | |
| $e,\mu$ | 9 | 0.04 | 0.01 |
| This work | | $-0.04\pm0.07$ | $-0.06\pm0.07$ |
| | | $\Delta R_n$ (fm) | |
| 79-MeV $\alpha$ | 10 | | $0.08\pm0.08$ |
| 1-GeV $p$ | 11 | $0.10\pm0.02$ | $0.16\pm0.02$ |
| This work | | $0.09\pm0.05$ | $0.14\pm0.05$ |

calculation.[12] The curves labeled Kisslinger,[5] Laplacian,[13] and separable[14] are optical-model calculations. These three models differ in their assumptions about the off-shell behavior of the $\pi$-nucleon $t$ matrix, and the corresponding potentials have substantially different forms. In spite of this, the various calculations differ by less than 20 mb for energies above 140 MeV. At lower energies where the nucleus is no longer black to pions a substantial degree of model dependence is observed. For this reason only the data points at 140 MeV and above were used to obtain the best-fit $\Delta R$ values.

At the present time it is still unclear whether the optical model accurately predicts total cross sections for energies near the (3, 3) resonance. However, this is not a serious problem for our analysis because the predicted total cross section differences are extremely insensitive to changes in the potentials.[15] For example, if one reduces the strength of the potential by a factor of 2, $\Delta\sigma_T$ changes by less than 10 mb for energies above 125 MeV. This insensitivity is a consequence of the strong pion abosrption. Glauber calculations show that near the resonance, the interactions which contribute to $\Delta\sigma_T$ occur where the density is very low (typically 10% of the central density). Thus, $\Delta\sigma_T$ is insensitive to the form of the potential in the nuclear interior. In particular, terms

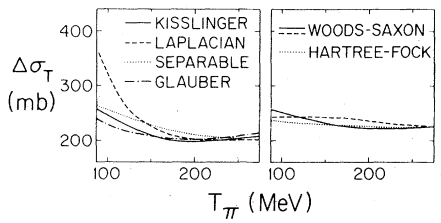


FIG. 2. Calculated total cross section differences for $\pi^-$ on $^{48}$Ca and $^{40}$Ca. The predictions of four $\pi$-nucleus interaction models are shown in (a). The calculations in (b) were obtained using the Kisslinger model with a variety of density functions which have the rms radii.

in the potential which are nonlinear in the density have little effect on the cross section differences.

Although we have used the $\Delta\sigma_T$ measurements to deduce values of $\Delta R_n$ and $\Delta R_p$, we do not wish to imply that the total cross sections rigorously depend only on the rms radii. The best-fit values of $\Delta R$ depend, to some extent, on the functional form of the densities. However, if we restrict ourselves to density functions which are physically reasonable (i.e., consistent with well established properties of nuclei), then the total cross sections are nearly identical for all density distributions which have the same rms radii. Kisslinger optical-model calculations obtained with a variety of density functions (all of which have the same rms radii) are shown in Fig. 2(b). For the dotted curve we used density distributions obtained from a Hartree-Fock calculation.[16] The solid curve was calculated using Woods-Saxon densities which closely match the Hartree-Fock densities. The dashed curves were obtained by increasing the 90–10% skin thickness for the $^{48}$Ca neutron distribution by 0.2 fm. For energies above 125 MeV, the various calculations differ by less than 15 mb.

The errors quoted for $\Delta R_p$ and $\Delta R_n$ in Table I include systematic as well as statistical errors. In particular, we have included uncertainties which arise from the Coulomb-nuclear interference correction (± 5 mb), pion decay and multiple scattering (± 5 mb), the extrapolation to $\Omega = 0$ (± 15 mb), the model dependence illustrated in Fig. 2(a) (± 10 mb), and the uncertainty in the functional form of the density (± 10 mb). The various contributions have been added in quadrature.

The values of $\Delta R_p$ obtained in the present experiment agree reasonably well with the results of electron scattering and muonic x-ray experiments[9] (see Table I). This gives us confidence that our treatment of the data and our estimate of the errors are reasonable. In Table I, one also sees that our values of $\Delta R_n$ are in good agreement with the results of recent experiments employing $\alpha$ particles[10] and high-energy protons.[11]

For $^{48}$Ca-$^{40}$Ca it is interesting to compare the experimental values of $\Delta R_n$ with the predictions obtained from Hartree-Fock theory.[17] The calculated values are typically near 0.25 fm, which is somewhat larger than the experimental result. This discrepancy is significant since a 0.1-fm decrease in the rms radius corresponds to nearly a 10% increase in the central density. A change of this magnitude would presumably require significant modifications in the Hartree-Fock calculations. Of course, the possibility that the experimental values of $\Delta R_n$ are in error cannot be ruled out, particularly since each of the experiments relies on a strong-interaction model to extract $\Delta R_n$. However, one should keep in mind that the proton, $\alpha$ particle, and pion experiments all give essentially the same result, even though different projectiles and models were used in each case. This fact provides evidence that the experimental values of $\Delta R_n$ are probably correct.

The authors wish to thank the staff at LAMPF for their assistance in executing this experiment.

---

*Work supported in part by the U. S. Energy Research and Development Administration.

[1]R. L. Burman, R. L. Fulton, and M. Jakobson, Nucl. Instrum. Methods 131, 29 (1975).

[2]See for example J. P. Stroot, Los Alamos Scientific Laboratory Report No. LA-5443-C, 1973 (unpublished), p. 1.

[3]B. A. Leontic and J. Teiger, Brookhaven National Laboratory Report No. BNL 50031, 1966 (unpublished).

[4]The Coulomb-nuclear interference corrections were calculated with the Kisslinger model. For energies above 125 MeV, those corrections are typically 5 mb.

[5]L. S. Kisslinger, Phys. Rev. 98, 761 (1955).

[6]In all of the optical-model calculations presented here, the $t$ matrix is transformed from the $\pi$-nucleon to the $\pi$-nucleus center-of-mass system as described in E. Kujawski and G. A. Miller, Phys. Rev. C 9, 1205 (1974).

[7]The $\pi$-$N$ phase shifts of L. D. Roper, R. M. Wright, and B. T. Feld, Phys. Rev. 138, B190 (1965) were used for most of the calculations. Other phase-shift sets produce results which are indistinguishable except at very low energies.

[8]One may also evaluate $\Delta R_n$ by fixing the proton radii at values obtained from electron scattering and muonic x-ray experiments. Using this method we obtain $\Delta R_n(^{48}\text{Ca}\text{-}^{40}\text{Ca}) = 0.11 \pm 0.05$ fm and $\Delta R_n(^{44}\text{Ca}\text{-}^{40}\text{Ca}) = 0.06 \pm 0.05$ fm.

[9]R. F. Frosch *et al.*, Phys. Rev. 174, 1380 (1968); R. D. Ehrlich, Phys. Rev. 173, 1088 (1968). The charge radii from the above papers were corrected for the finite proton and neutron sizes as described by W. Bertozzi, J. Friar, J. Heisenberg, and J. W. Negele, Phys. Lett. 41B, 408 (1972).

[10]G. M. Lerner *et al.*, Phys. Rev. C 12, 778 (1975).

[11]G. D. Alkhazov *et al.*, Phys. Lett. 57B, 47 (1975); G. D. Alkhazov *et al.*, Nucl. Phys. A274, 443 (1976).

[12]H. O. Meyer, to be published.

[13]H. K. Lee and H. McManus, Nucl. Phys. A167, 257 (1971); G. Fäldt, Phys. Rev. C 5, 400 (1972); J. H. Koch and M. Sternheim, Phys. Rev. C 6, 1118 (1972).

[14]R. H. Landau, S. C. Phatak, and F. Tabakin, Ann. Phys. (N.Y.) 78, 299 (1973); S. C. Phatak, F. Tabakin,

and R. H. Landau, Phys. Rev. C 7, 1803 (1973). The form of the $\pi$-$N$ $t$ matrix was that of J. Londergan, K. McVoy, and E. Moniz, Ann. Phys. (N.Y.) 86, 147 (1974).

[15]Throughout this paper, we assume that one should use the same optical-model formulation for all three Ca isotopes. If this assumption is not made (e.g., if one uses different models for $^{40}$Ca and $^{48}$Ca) it is possible to produce large changes in the calculated $\Delta\sigma_T$ values.

[16]J. W. Negele and D. Vautherin, Phys. Rev. C 5, 1472 (1972); J. W. Negele, private communication.

[17]See Ref. 13 and references cited in Ref. 15 and in R. C. Barrett, Rep. Prog. Phys. 37, 1 (1974).

# Excited-State Spectroscopy of Molecules Using Opto-acoustic Detection

C. K. N. Patel, R. J. Kerl, and E. G. Burkhardt
*Bell Telephone Laboratories, Inc., Murray Hill, New Jersey 07974, and Holmdel, New Jersey 07733*

(Received 21 March 1977)

Opto-acoustic high-resolution spectroscopy of the $v=1\rightarrow 2$ vibrational-rotational transitions of the $^2\Pi_{1/2}$ and $^2\Pi_{3/2}$ states of NO is reported. Accurate frequencies for the $1\rightarrow 2$ band centers for both the $^2\Pi_{1/2}$ and $^2\Pi_{3/2}$ states are obtained. The opto-acoustic detection technique has allowed Zeeman spectroscopy of the excited-state transitions.

We report excited-state spectroscopy of the $v=1$ vibrational levels of the $^2\Pi_{1/2}$ and $^2\Pi_{3/2}$ states of NO carried out using opto-acoustic (OA) detection in conjunction with a tunable spin-flip Raman (SFR) laser. We have determined the $v=1\rightarrow 2$ band-center frequencies for both substates of NO, and have carried out preliminary Zeeman spectroscopy of the transitions. We also report the measurements of $\Lambda$ doubling in the $^2\Pi_{1/2}$, $v=1\rightarrow 2$ transitions of NO.

OA spectroscopy has been used[1] for a number of experiments where extremely small absorptions in gaseous samples have been measured. This technique has recently[2] been refined to improve the sensitivity as well as to allow operation at lower gas pressures. The miniaturization of the OA cells without any loss of signal allows utilization of very short absorption cells which can be subjected to strong uniform magnetic fields for Zeeman spectroscopy. The new ability to measure absorption coefficient as small as $10^{-10}$ cm$^{-1}$ when OA detection technique is employed together with a low-field SFR laser[3] points to numerous studies of gaseous spectra.

The experimental approach for studying the $v=1\rightarrow 2$ vibrational-rotational (v-r) transitions of NO involves the optical excitation[4,5] of the molecules from $v=0$ to the $v=1$ vibrational level using a fixed-frequency CO-laser[6] line $P_{8\text{-}7}(11)$ at 1917.8611 cm$^{-1}$ ($h\nu_2$). The molecules are examined spectroscopically with tunable infrared radiation ($h\nu_1$) obtained from an InSb SFR laser pumped with another CO-laser line[6] $P_{8\text{-}7}(16)$ at 1897.6545 cm$^{-1}$ which travels collinearly with the fixed-frequency CO-laser radiation. Both of these radiations are focused into a 1-cm OA cell using a 20-cm-focal-length lens. Typical NO pressures of 200 mTorr to 2 Torr were used.

Recently Guerra, Sanchez, and Javan[5] have studied the $^2\Pi_{1/2}$, $v=1\rightarrow 2$ transitions using a conventional absorption measurement technique by having the fixed-frequency CO-laser beam as well as the tunable SFR laser radiation travel collinearly through a 60-cm optical wave guide for obtaining a long interaction length. The OA technique utilized here requires only a 1-cm path length, and has allowed the measurements of both the $^2\Pi_{1/2}$ and $^2\Pi_{3/2}$, $v=1\rightarrow 2$ transitions. In our experiments, the two-photon absorption studies can be carried out in a controlled fashion and without the near vicinity of the walls (0.6 mm diam, in Ref. 5) which may cause rapid de-excitation of the NO molecules excited to $v=1$ vibrational level by the fixed-frequency CO laser ($h\nu_2$) and thereby reduce the absorption of the desired $v=1\rightarrow 2$, v-r transitions. In addition, the walls would also cause dephasing collisions which would increase the homogeneous width measured by saturation spectroscopy or two-photon Doppler-free spectroscopy.

Figure 1(a) shows an OA absorption signal as a function of the magnetic field, $B$, tuning the SFR laser frequency, $h\nu_1$, for a NO pressure of 500 mTorr without the presence of the fixed frequency $h\nu_2$. In this trace four lines are identified as arising from the $R(\frac{7}{2})$ and $R(\frac{9}{2})$, $^2\Pi_{1/2}$ and $^2\Pi_{3/2}$, $v=0\rightarrow 1$ transitions[7,8] at $B\approx 1543$, 1665, 2963, and 3049 G, respectively. (We will use short-hand notation $R_{0\text{-}1}(J)_{\pi_{1/2}}$, etc. to denote the various NO transitions in the remaining text). Because the